Nuclear Instruments and Methods in Physics Research B 317 (2013) 565–569

Contents lists available at SciVerse ScienceDirect

Nuclear Instruments and Methods in Physics Research B

journal homepage: www.elsevier.com/locate/nimb

The Collinear Resonance Ionization Spectroscopy (CRIS) experimental setup at CERN-ISOLDE ☆

T.E. Cocolios [a,b,*], H.H. Al Suradi [c], J. Billowes [a], I. Budinčević [d], R.P. de Groote [d], S. De Schepper [d], V.N. Fedosseev [e], K.T. Flanagan [a], S. Franchoo [f], R.F. Garcia Ruiz [d], H. Heylen [d], F. Le Blanc [f,1], K.M. Lynch [a,b], B.A. Marsh [e], P.J.R. Mason [g,2], G. Neyens [d], J. Papuga [d], T.J. Procter [a], M.M. Rajabali [d,3], R.E. Rossel [e,h], S. Rothe [e,h], G.S. Simpson [i], A.J. Smith [a], I. Strashnov [a], H.H. Stroke [j], D. Verney [f], P.M. Walker [g], K.D.A. Wendt [h], R.T. Wood [g]

[a] School of Physics and Astronomy, University of Manchester, Manchester M13 9PL, United Kingdom
[b] ISOLDE, PH Department, CERN, CH-1211 Geneva-23, Switzerland
[c] University of Sharja, Sharja, United Arab Emirates
[d] Instituut voor Kern- en Stralingsfysika, KU Leuven, B-3001 Leuven, Belgium
[e] EN Department, CERN, CH-1211 Geneva-23, Switzerland
[f] Institut de Physique Nucléaire d'Orsay, F-91406 Orsay, France
[g] Centre for Nuclear and Radiation Physics, University of Surrey, Guilford GU2 7XH, United Kingdom
[h] Institut für Physik, Johannes Gutenberg Universität, D-55099 Mainz, Germany
[i] LPSC, F-38026 Grenoble Cedex, France
[j] New York University, New York, NY 10003, United States

ARTICLE INFO

Article history:
Received 11 March 2013
Received in revised form 27 May 2013
Available online 4 July 2013

Keywords:
Laser spectroscopy
Hyperfine structure
Isotope shift
Ion beam purification
Radioactive decay spectroscopy

ABSTRACT

The CRIS setup at CERN-ISOLDE is a laser spectroscopy experiment dedicated to the high-resolution study of the spin, hyperfine structure and isotope shift of radioactive nuclei with low production rates (a few per second). It combines the Doppler-free resolution of the in-flight collinear geometry with the high detection efficiency of resonant ionisation. A recent commissioning campaign has demonstrated a 1% experimental efficiency, and as low as a 0.001% non-resonant ionisation. The current status of the experiment and its recent achievements with beams of francium isotopes are reported. The first identified systematic effects are discussed.

1. Introduction

Laser spectroscopy of radioactive atoms provides ground-state nuclear properties without any nuclear model assumptions [1,2]. It has therefore attracted a lot of interest in the recent years [3,4] and the techniques are being pushed to their limits to study the most exotic systems.

In general, the collinear laser spectroscopy technique uses beams produced at on-line facilities where the ions are mass separated and delivered either continuously or alternatively in bunches to the experimental setup. The beam may be neutralised in an alkali vapour upon entering the atom/laser interaction region where the atom beam is overlapped by a co-propagating laser beam. The excited atoms decay and the resonantly scattered photons are detected with photomultipliers. The acceleration of the beam provides a reduction of the velocity distribution of the ions, resulting in a Doppler compression of the resolution down to the natural line width. This technique has benefited, in recent years, from the use of bunched beams [5,6] and has reached a sensitivity down to 100 ions per second under optimum conditions [7], though a more typical required rate is 10,000 ions per second [3].

In-source laser spectroscopy is an alternative to the collinear laser spectroscopy technique and has gained particular interest in the last decade [8]. The isotopes of interest are resonantly ionised within the ion source with a series of resonant transitions, one of

* Corresponding author at: School of Physics and Astronomy, University of Manchester, Manchester M13 9PL, United Kingdom. Tel.: +44 1612754281; fax: +44 1612755509.
E-mail address: Thomas.Elias.Cocolios@cern.ch (T.E. Cocolios).
[1] Present address: IPHC, Strasbourg, France.
[2] Present address: STFC Daresbury Laboratory, Daresbury, United Kingdom.
[3] Present address: TRIUMF, Vancouver, BC, Canada.

0168-583X/$ - see front matter © 2013 The Authors. Published by Elsevier B.V. All rights reserved.
http://dx.doi.org/10.1016/j.nimb.2013.05.088

which is scanned across the resonance, mass separated and delivered to a counting station. The high efficiency of ion counting and the possibility of decay tagging has made this technique very powerful and has allowed the study of isotopes with production rates below 1 atom per second [9–12]. The spectroscopic resolution is dependent upon the ion source conditions (temperature, pressure, divergence) and is typically 100–1000 times lower than in collinear laser spectroscopy, although continuous improvements are ongoing [13].

The Collinear Resonance Ionisation Spectroscopy (CRIS) technique was proposed as a means of benefiting from both techniques [14]. The ion beam is prepared and delivered to the experiment as in collinear laser spectroscopy. The atom beam is then overlapped with additional laser beams for efficient ionisation. The ionised beam is finally deflected towards a high-efficiency counting station.

The first demonstration of this technique suffered however from a low duty cycle associated with overlapping a continuous ion beam with a pulsed laser system [15], resulting in an efficiency of 0.001%. Subsequent tests performed at the University of Jyväskylä with bunched beams and synchronised pulsed lasers achieved a high efficiency but suffered from bad vacuum conditions resulting in a high background rate from non-resonant collisional re-ionisation [6,16–18].

2. The CRIS setup at ISOLDE

The new CRIS setup at CERN ISOLDE has been designed to overcome the shortcomings of the previous applications of this technique. The three components of the setup are the ion beam line, the laser system, and the detection chamber.

2.1. The CRIS beam line

The radioactive beam is produced upon the impact of the CERN PSBooster proton beam onto the ISOLDE target [19]. The nuclear-reaction products diffuse and effuse to an ion source, the ions are accelerated to 30–50 keV, mass separated in the high-resolution separator magnets HRS [20], cooled and bunched in a gas-filled radio-frequency quadrupole linear Paul trap (ISCOOL) [21] and delivered to the experimental setup.

A detailed description of the CRIS beam line can be found in Ref. [22]. Its most important features and characteristics are presented in this section and can be seen in Fig. 1. The ion bunch is deflected to the laser axis to be overlapped. It is then neutralised in a potassium-filled charge-exchange cell. The charge-exchange cell chamber may be biased to Doppler tune the bunch onto resonance. The potassium vapour is maintained at a temperature near 150 °C and produces a background pressure of the order of 10^{-6} mbar.

The neutral atom bunch is then directed through a differential pumping region while the non-neutralised component is deflected within the differential pumping region. The atom bunch is temporally overlapped with the laser pulse in the interaction region, where the pressure is maintained under 10^{-8} mbar, in order to minimise non-resonant collisional ionisation. The axial overlap is adjusted with ion optic electrodes upstream of the charge-exchange cell, while the longitudinal overlap is adjusted by synchronising the laser pulses with the bunch release from ISCOOL. In the study of the francium isotopes, the atom bunch width was found to be ~ 2 μs, which is well contained within the length of the interaction region (1.5 m).

At the end of the interaction region, the re-ionised atoms are deflected to the decay-spectroscopy station (DSS) to be counted with either a micro-channel plate (MCP) detector or an α-decay spectroscopy setup.

2.2. The laser system

The francium atoms are ionised in a two-step process, with a resonant transition from the $7s^2S_{1/2}$ atomic ground state to the $8p^2P_{3/2}$ state at 23,658.306 cm^{-1}, and a non-resonant excitation across the ionisation potential with a 1064 nm laser pulse.

The full laser system can be seen on Fig. 2. The 422.7 nm laser light is provided by one of the RILIS tunable Ti:Sapphire (Ti:Sa) laser [23], which was operated in narrow line-width mode [24]. The Ti:Sa laser is pumped with a frequency doubled Nd:YAG laser, operating at 10 kHz pulse repetition rate. The fundamental output of the Ti:Sa laser is frequency doubled in a BBO crystal. The laser light is delivered to the CRIS experimental setup via a 35 m-long optical fibre. The ability to scan this laser system has been improved recently by the implementation of a remote control system with a built-in stability control system [25]. The bandwidth of the fundamental laser light was typically 1 GHz.

The second step used the fundamental output of a Nd:YAG laser at 30 Hz repetition rate. The two lasers are synchronised temporally and the time overlap is monitored with a photodiode placed downstream of the interaction region. The 10 kHz signal was used as the master trigger for the experiment.

The two laser pulses are merged spatially on a launch platform in front of the beam line and overlapped with the ion/atom beam

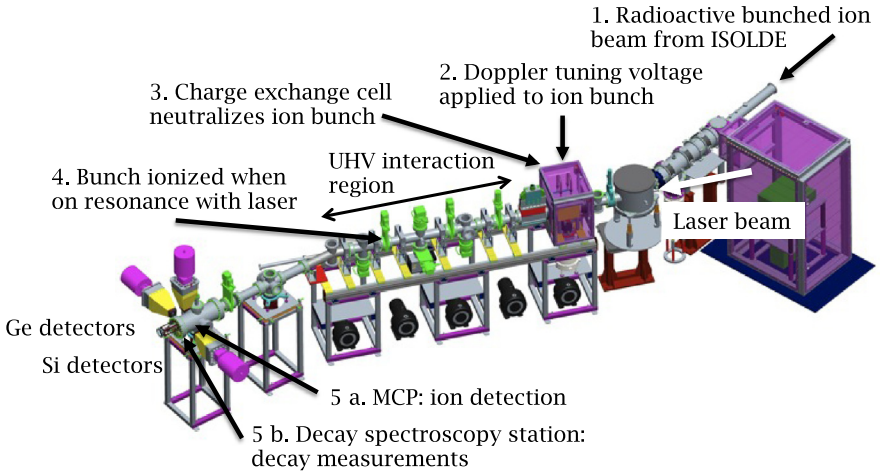

Fig. 1. Layout of the CRIS beam line. The ion and laser beams travel from right to left through the charge exchange cell, the interaction region, and finally to the DSS.

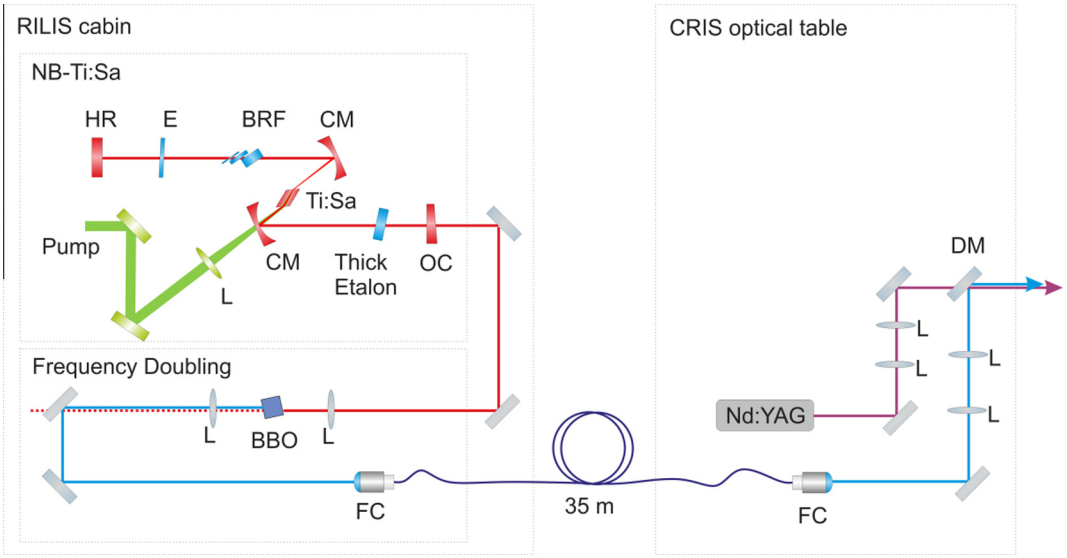

Fig. 2. Layout of the laser system for the 2012 CRIS campaign. The 10 kHz-pulsed tunable-frequency laser light at 422.7 nm was provided by the RILIS team [23,24] and transported to the CRIS optical bench via a 35 m-long optical fibre. The tunable first step laser is overlapped with the fundamental infra-red light from a 30 Hz Nd:YAG laser at 1064 nm. Both laser beams are reflected to the beam line and overlapped with the atoms in the interaction region. (For interpretation of the references to colour in this figure caption, the reader is referred to the web version of this article.)

axis prior to the charge exchange cell. The differential pumping apertures are used as guides for the laser beam alignment. The final atom/laser beam overlap adjustments are performed on-line using the intensity and time profile of the resonance signal.

2.3. The ion detection setups

The re-ionised atoms are deflected into the DSS and impinge upon a biased copper plate. Secondary electrons are emitted from the ion impacts and are guided via an electric field gradient to the surface of an MCP detector (see Fig. 3). The signal from the MCP is digitised and processed via a LeCroy WavePro Zi 2.5 GHz bandwidth oscilloscope. Only signals in time coincidence with the expected arrival of the re-ionised atoms are recorded. The total efficiency of ion counting has been estimated on-line to be >30%.

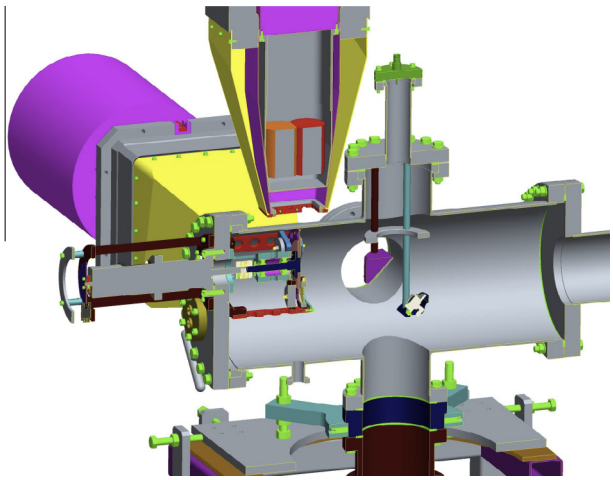

Fig. 3. MCP for secondary electron emission detection in the CRIS DSS chamber. The beam enters the chamber from the right side, hits the biased copper dynode (centre of the picture, purple) and are transported to the MCP with a guiding electric field. (For interpretation of the references to colour in this figure caption, the reader is referred to the web version of this article.)

Possible sources of background may arise from radioactivity on the copper plate, dark counts of the MCP, or noise on the electronic signals. The radioactivity on the plate is dependent upon the implantation rate from the beam and the half-life of the isotopes along the decay chain. The experimental protocol was thus designed to avoid intense beam implantation and to keep the strongest activity from contaminating the setup. Decay periods were also considered to let the activity on the plate reduce in preparation for cases needing high sensitivity.

The MCP dark count rate is low (1 count per second) and randomly distributed in time. The probability of observing a dark count event in the acquisition window (10 μs window at 30 Hz) is therefore 3×10^{-4}. This bunching compression of the background rate reduces the radioactivity-related background as well.

Finally, the noise on the electronic signal has been the subject of an extensive investigation. The surrounding electric and electronic components have all been controlled and selected in order to minimise their impact.

The re-ionised beam may also be deflected into the α-decay spectroscopy setup. A complete description of the decay setup can be found in Ref. [26–28]. The sample holder and silicon detector assembly can be seen in Fig. 4.

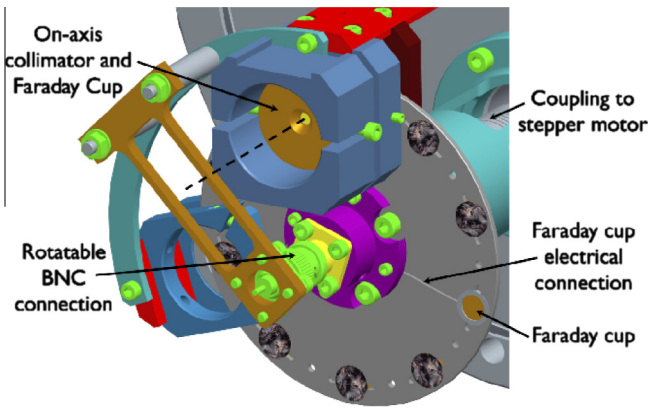

Fig. 4. Layout of the CRIS Decay Spectroscopy Station.

The beam is implanted through a 4 mm aperture onto a 20 μg/cm^2 carbon foil [29] mounted on a rotatable wheel with 9 sample holders and a Faraday cup. The implantation site is surrounded by two silicon detectors (thickness 300 μm) to measure the energy of charged particles emitted during the radioactive decay of the implanted sample. The detector upstream of the implantation sample has an aperture of 4 mm to let the ion beam through. A collimator prevents direct deposition on the back of the annular detector. Two additional silicon detectors surround an off-axis position to study longer-lived isotopes in pure decay conditions or to monitor the remaining activity on the carbon foils.

The solid-angle coverage of the on-axis detectors has been simulated to collect 68% of the charged particles. The line profiles have also been simulated, accounting for the penetration of the foil thickness at different angles using the SRIM simulation package [30].

Up to three high-purity germanium detectors can be placed around the DSS to observe the γ rays in coincidence with the charged particles. An in-depth discussion on the γ-ray intensity attenuation and efficiency can be found in Ref. [26].

3. Results of the 2012 campaign

In the course of the 2012 campaign, the hyperfine structure of the isotopes $^{202–207,211,219–221,229,231}$Fr and of isomers in ^{202,204,206,218}Fr have been studied at the CRIS setup over two experimental runs in August [17] and October. More information on the scientific results may be found in forthcoming publications.

3.1. Performance

A representative hyperfine spectrum of ^{221}Fr is shown in Fig. 5. Each frequency point is sampled for 10 s for isotopes with reasonably high or continuous production rates, or for a full PSBooster supercycle (36–54 s) for weakly produced isotopes which production is highly correlated to the proton impact on target. The experimental conditions were optimised on the ^{221}Fr resonance: the spatial and temporal overlap of the laser pulses and atom bunches, the charge exchange cell temperature, and the laser power in the resonant and non-resonant steps.

A neutralisation efficiency of 50% was achieved using potassium. The total re-ionisation efficiency during the campaign, including the transport from ISCOOL, neutralisation, laser ionisation, and detection, reached $\epsilon_r > 1\%$. The non-resonant equivalent efficiency was determined to be $\epsilon_n < 0.001\%$ while operating at a pressure of 8×10^{-9} mbar in the interaction region. For a beam contamination of 50% from the ion source (e.g. to disentangle two isomers), this would correspond to $(\epsilon_r - \epsilon_n)/\epsilon_r > 99.9\%$ beam purity at the exit of the CRIS setup.

The most exotic case studied in the course of the 2012 campaign was ^{202}Fr, with a yield of 100 ions/μC. The essentially background-free conditions permitted the identification of the scanning regions of interest in 5 min, contributing to the overall campaign success.

3.2. Systematic analysis

As the technique of in-flight laser ionisation has not yet been thoroughly investigated and considering the recent challenges that the in-source laser ionisation technique has been confronted with [31–33], a systematic investigation of the results is crucial.

We have therefore repeatedly remeasured the hyperfine spectrum of ^{221}Fr through the course of the campaign, as well as its isotope shift to ^{207,211,220}Fr. We report here on the extraction of the magnetic dipole moment from each of those four isotopes. A total of 29 data points are available.

The hyperfine spectra, as shown in Fig. 5, have been analysed by fitting Voigt profiles, from which it was finally determined that the line shape is dominated by the Gaussian contribution from the narrow-band Ti:Sa laser (FWHM 1.5 GHz). From the combination of the nuclear spins to the electron angular momentum, two groups of peaks are expected, consisting of 1–3 peaks depending upon the nuclear spin. Those are however not resolved. The spectra are then fitted with the 3–6 required components; their position being determined relatively with respect to the transition centre of gravity using the atomic ground-state hyperfine parameter A_{gs} and the excited state hyperfine parameters A_{es} and B_{es}. The fit is found to be insensitive to the B_{es} parameter, this is therefore ignored. The resolution is not sufficient to extract the A_{es} parameter: it was related to A_{gs} by imposing a constant ratio, and assuming that the experimental conditions were not sensitive to the hyperfine anomaly. The relative intensity of the two envelopes are kept independent, however the relative intensity of the peaks within each envelope is assumed to be that of standard angular momentum coupling. Although this is known to be incorrect [32,34], it is the most realistic estimate currently available.

The moments are compared to the literature values and their ratios are shown in Fig. 6. A scatter of 0.7% is found around 0.999 and is considered as the experimental uncertainty of the 2012

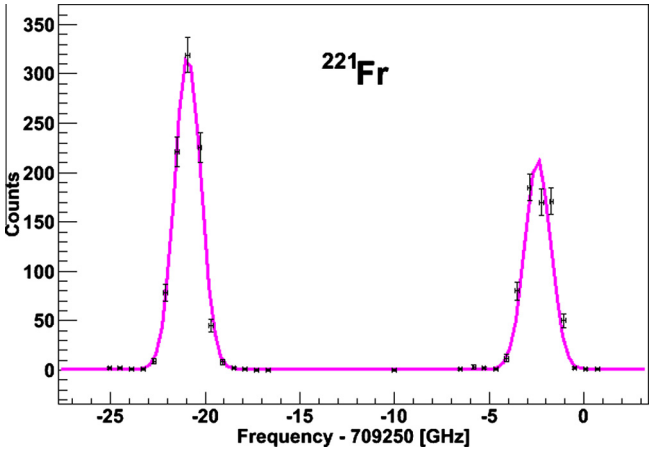

Fig. 5. Spectrum of ^{221}Fr. Each point is sampled for 10 s.

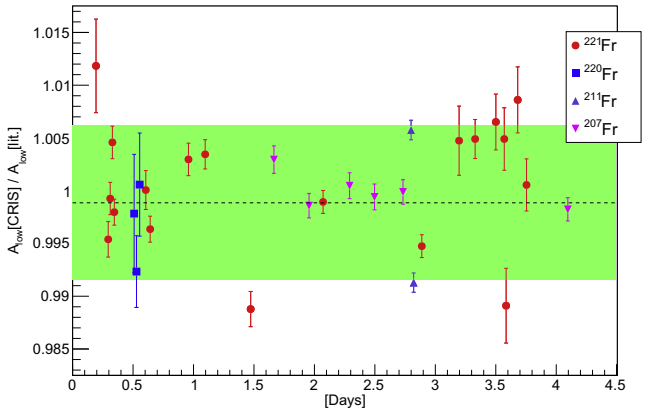

Fig. 6. Distribution of the CRIS hyperfine parameter A_{gs} for the atomic ground state of francium in ^{207,211,220,221}Fr with respect to the literature values. The error bars reflect only the statistical uncertainty of each measurement. The results scatter by 0.7% around the literature values (shaded area).

campaign using the current laser system, corresponding to an absolute error of about 30–40 MHz on the hyperfine parameter A_{gs}. This scatter is believed to be mostly due to the limited resolution of the laser system used in this campaign. This corresponds to a significant improvement with respect to the several 100 MHz uncertainty reported from previous campaigns [35].

3.3. α-decay tagging

Beams that consist of several isomers of an isotope present the added difficulty that their respective components cannot be identified with the MCP. Instead, the beam for each component is delivered to the DSS to tag them according to the characteristic pattern of their decay [28].

In the case of the francium isotopes, the beams may contain up to 3 states with similar half-lives and production rates. Several hyperfine components are accordingly observed in the MCP scan data. The beam re-ionised for those respective components can then be delivered to the DSS, yielding the different α-decay energy spectra from which the respective nuclear states can be identified.

Decay spectroscopy data was also acquired to study some of these isotopes in unprecedented clean conditions. These results are reported in a forthcoming publication.

4. Conclusions

The CRIS setup has been built at CERN ISOLDE in order to study the ground-state properties of very exotic nuclei. The successful 2012 campaign has demonstrated an efficiency better than 1% for a background rate up to 0.001%. The ground state of 13 isotopes and isomeric states in 4 isotopes of francium have been studied in near background-free conditions, with intensities as low as 100 ions/μC. The α-decay tagging and beam purification have also been demonstrated at the DSS.

The first systematic analysis of magnetic dipole moments has shown no systematic shift and concluded in an uncertainty of 0.7%.

The CRIS setup will be improved in the coming years in terms of higher efficiency (beam transport, detection efficiency, laser power), increased resolution (continuous wave laser operation, reliable Doppler tuning), and reduced background rate (better vacuum with Getter material and additional differential pumping). The range of applicability shall also be expanded with the introduction of additional laser systems for 3-step ionisation schemes, using either field ionisation of high-lying Rydberg states, or alternatively via auto-ionising states.

Finally, the success of this technique with small sample size opens new possibilities for beam manipulation and purification at radioactive ion beam facilities and for trace analysis.

Acknowledgements

We would like to thank the ISOLDE collaboration and technical teams for providing the beams and the GSI target group for manufacturing the carbon foils. This work was supported by the U.K. Science and Technology Facilities Council (consolidated grant ST/F012071/1 and continuation grant ST/J000159/1), by FWO-Vlaanderen (Belgium), by GOA/2004/03 (BOF-KU Leuven), by the IUAP – Belgian State Belgian Science Policy – (BriX network P7/12), and by the European Commission within FP7 (ENSAR No. 262010). Contributions from Ed Schneiderman to the Physics Department of NYU are greatly appreciated.

References

[1] K. Blaum, J. Dilling, W. Nörtershäuser, Physica Scripta T152 (2013) 014017.
[2] B. Cheal, T.E. Cocolios, S. Fritzsche, Journal of Physics G 39 (2012) 125101.
[3] B. Cheal, K.T. Flanagan, Journal of Physics G 37 (2010) 113101.
[4] K.T. Flanagan, AIP Conference Proceedings 1377 (2011) 38–45.
[5] P. Campbell et al., Laser spectroscopy of cooled zirconium fission fragments, Physical Review Letters 89 (2002) 082501.
[6] P. Campbell, A. Nieminen, et al., European Physics Journal A 15 (2002) 45.
[7] K.T. Flanagan et al., Physical Review A 86 (2012) 042501.
[8] V.N. Fedosseev, Y. Kudryavtsev, V.I. Mishin, Physica Scripta 85 (2012) 058104.
[9] H. De Witte et al., Physical Review Letters 98 (2007) 112502.
[10] M.D. Seliverstov et al., European Physics Journal A 41 (2009) 315–321.
[11] T.E. Cocolios, M.D. Seliverstov, et al., Physical Review Letters 106 (2011) 052503.
[12] M.D. Seliverstov, T.E. Cocolios, et al., Physics Letters B 719 (2013) 362–366.
[13] Y. Kudryavtsev, R. Ferrer, M. Huyse, P. Van den Bergh, P. Van Duppen, Nuclear Instruments and Methods B 297 (2013) 7–22.
[14] Y.A. Kudriavtsev, V.S. Letokhoov, Applied Physics B 29 (1982) 219.
[15] C. Schultz et al., Journal of Physics B 24 (1991) 4831.
[16] K.T. Flanagan, Ph.D. thesis, University of Manchester, 2004.
[17] K.T. Flanagan, Acta Physica Polonica B 44 (2013) 627.
[18] K.T. Flanagan, World Scientific Publishing Co., Conference Proceedings to the Sanibel Conference on Fission 2012 (2013) in review.
[19] E. Kugler, Hyperfine Interactions 129 (2000) 23–42.
[20] T.J. Giles, R. Catherall, F. Fedosseev, U. Georg, E. Kugler, J. Lettry, M. Lindroos, Nuclear Instruments and Methods B 204 (2003) 497–501.
[21] E. Mané et al., European Physics Journal A 42 (2009) 503.
[22] T.J. Procter et al., Journal of Physics: Conference Series 381 (2012) 012070.
[23] S. Rothe, B.A. Marsh, C. Mattolat, V.N. Fedosseev, K. Wendt, Journal of Physics: Conference Series 312 (2011) 052020.
[24] S. Rothe et al., Nuclear Instruments and Methods B (2013) these proceedings.
[25] R.E. Rossel et al., Nuclear Instruments and Methods B 317 (2013) 557–560.
[26] M.M. Rajabali, K.M. Lynch, T.E. Cocolios, et al., Nuclear Instruments and Methods A 707 (2013) 35–39.
[27] K.M. Lynch, M.M. Rajabali, et al., Journal of Physics: Conference Series 381 (2012) 012128.
[28] K.M. Lynch, T.E. Cocolios, M.M. Rajabali, Hyperfine Interactions 216 (2013) 95–101.
[29] B. Lommel, W. Hartmann, B. Kindler, J. Klemm, J. Steiner, Nuclear Instruments and Methods A 480 (2002) 199–203.
[30] J.F. Ziegler, J.P. Biersack, Available from: <http://www.srim.org/>.
[31] T.E. Cocolios et al., Physical Review Letters 103 (2009) 102501.
[32] T.E. Cocolios et al., Physical Review C 81 (2010) 014314.
[33] P. Vingerhoets, K.T. Flanagan, et al., Physics Letters B 703 (2011) 34–39.
[34] S. Gheysen, G. Neyens, J. Odeurs, Physical Review C 69 (2004) 064310.
[35] T.J. Procter, K.T. Flanagan, Hyperfine Interactions 216 (2013) 89–93.